

D101 is critical for the function of AttJ, a repressor of quorum quenching system in *Agrobacterium tumefaciens*

Chao Wang^{1,2}, Chunlan Yan³, Yong-Gui Gao^{1,4*},
and Lian-Hui Zhang^{1,5*}

¹Institute of Molecular and Cell Biology, 61 Biopolis Drive, 138673, Singapore

²Division of Cellular & Molecular Research, National Cancer Centre Singapore, 11 Hospital Drive, 169610, Singapore

³College of Life Science, South-Central University for Nationalities, 430074, P. R. China

⁴School of Biological Sciences, Nanyang Technological University, 60 Nanyang Drive, 637551, Singapore

⁵Guangdong Province Key Laboratory of Microbial Signals and Disease Control, South China Agricultural University, 510642, P. R. China

(Received Feb 26, 2015 / Revised Jun 3, 2015 / Accepted Jun 29, 2015)

The quorum quenching system of *Agrobacterium tumefaciens* is specifically activated upon entering the stationary phase. Evidence has shown that this system includes two key components: the IclR-type transcriptional factor AttJ (also named as BlcR) and the AHL-lactonase AttM (also named as BlcC). At exponential phase, AttJ binds to the promoter region of *attM* and thus suppresses the expression of *attM*. At stationary phase, however, the small molecule SSA directly binds to AttJ and relieves its inhibition of AttJ and thereby triggers the expression of *attM*. While the regulation of AttM has been extensively investigated, little is known about the regulation of AttJ. In this study, we demonstrated the D101 amino acid of AttJ is essential for the AttJ function. *In vitro*, the variant protein of AttJ_{D101H} appeared to be readily aggregated. *In vivo*, the D101H mutation in AttJ entirely abolished the inhibitory activity of AttJ and overexpressed *attM* in *A. tumefaciens* A6. In addition, D101H mutation led to an overexpression of *attJ*, indicating an auto-regulatory mechanism for the *attJ* regulation. Put together, these findings demonstrate that D101 is an important amino acid for the transcription activity of AttJ and the transcription of *attJ* is regulated by a negative feedback loop. These results expand previous biochemical characterization of AttJ and provide new mechanistic insights into the regulation of quorum quenching in *A. tumefaciens*.

Keywords: quorum sensing, autorepression, AHL-lactonase, γ -butyrolactone, IclR-type regulator, BlcR

Introduction

Quorum sensing (QS) is a widespread strategy for bacterial gene regulation via producing, secreting and perceiving diffusible signals. In the Gram-negative bacteria, the QS signals appeared to be N-acylhomoserine lactones (AHL) and regulated various biological functions ranging from virulence expression to antibiotic production (Waters and Bassler, 2005; Rutherford and Bassler, 2012). In *Agrobacterium tumefaciens*, the AHL signal has been identified as N-(3-oxo-octanoyl)-L-homoserine lactone (3OC8HSL), and the QS system has been shown to regulate the Ti plasmid replication and conjugation (Piper *et al.*, 1993; Zhang *et al.*, 1993; Pappas and Winans, 2003). Evidence has shown that the QS system in *A. tumefaciens* could be induced by plant opines, activated by the TraR-3OC8HSL complex, and suppressed by the antiactivator TraM (White and Winans, 2007). Recent evidence additionally showed the QS system of *A. tumefaciens* is also associated with the quorum quenching (QQ) system (Zhang *et al.*, 2002b), a mechanism for bacteria to switch off QS by destroying the QS signal (Dong *et al.*, 2000; Wang *et al.*, 2006b).

In *A. tumefaciens* A6, the QQ system contains two key components. One is *attM*, which encodes an AHL-lactonase for enzymatic digestion of 3OC8HSL. The other is *attJ*, which encodes a transcriptional factor for negative regulation of *attM*. Together with *attK* (also named as BlcA, encoding a succinic semialdehyde dehydrogenase) and *attL* (also named as BlcB, encoding a homolog of alcohol dehydrogenase), *attM* constitutes the *attKLM* operon which is transcribed from the *attK* promoter (Zhang *et al.*, 2002b). The *attJ* gene, on the other hand, locates adjacently but transcribes divergently with the *attKLM* operon. At exponential phase, AttJ switches off the QQ system by suppressing the *attKLM* transcription so that 3OC8HSL could accumulate up to initiate the QS system. At stationary phase, however, the repression of AttJ is somehow relieved and the transcription of *attM* is activated so that the QQ system could be active to terminate the QS system (Zhang *et al.*, 2002b). Studies have shown the QQ system is regulated by starvation stress. Knock-out of *relA*, a gene encodes the (p)ppGpp synthetase for bacterial stringent responses, abolished the stationary phase-dependent expression of *attM*. In addition, activation of QQ could be significantly postponed by supplementation of extra nutrient sources (Zhang *et al.*, 2004). Further evidence demonstrated that succinic semialdehyde (SSA), an important metabolite of GABA-shunt, also involves in the QQ regulation. By directly releasing the AttJ repressor from the *attK* promoter, SSA activates the expression of AttM and triggers the QQ system when bacteria encounter nutrient depletion

*For correspondence. (Y.G. Gao) E-mail: ygao@ntu.edu.sg / (L.H. Zhang) lianhui@imcb.a-star.edu.sg

(Wang et al., 2006b). In addition to SSA, gamma-aminobutyric acid (GABA), gamma-butyrolactone (GBL), and gamma hydroxy butyrate (GHB) are also suggested to regulate the QQ system in *A. tumefaciens*, possibly by conversion into the SSA ligand (Carlier et al., 2004; Chevrot et al., 2006; Wang et al., 2006b).

In the genome of *A. tumefaciens* C58, AttJ was annotated as a member of the IclR-like (isocitrate lyase regulator) regulators. In prokaryotes, the IclR-type regulators appeared to be widely conserved. Over 100 known members of the IclR family have been found in 44 species of bacteria and 2 archaea, with 9 IclR homologues in *Escherichia coli* alone (Zhang et al., 2002a). Typically, the IclR-type regulators contain a DNA binding domain in N-terminus and a ligand binding domain at C-terminus (Krell et al., 2006). Though directly acting on their cognate promoters, the IclR-type regulators could control various bacterial functions by activating or suppressing target genes (Grainger et al., 2004). These functions include the glyoxylate shunt in Enterobacteriaceae (Sunnarborg et al., 1990), multidrug resistance and degradation of aromatic compounds in soil bacteria (Bertani et al., 2001), virulence in phytopathogenic *Erwinia* sp. (Bell et al., 2004), and sporulation in *Streptomyces* (Molina et al., 2006). In *A. tumefaciens*, AttJ has been found to involve in QQ regulation and this finding adds a new dimension for the function of IclR-type regulators. At peptide level, AttJ shares 25% identity with IclR in *E. coli*, the prototype of IclR-family repressors. Tn5 inactivation of AttJ completely

abolishes the AHL signal accumulation and defects the Ti plasmid transfer in *A. tumefaciens* (Zhang et al., 2002b). In addition to the QQ regulation, AttJ has also been suggested to participate in the GBL assimilative pathway in *A. tumefaciens* (Carlier et al., 2004; Haudecoeur et al., 2009a). Crystal structure showed that attJ folds into the DNA-binding and ligand-binding domains and dimerizes via a α -helix region which links the two domains (Pan et al., 2011).

So far, it has been well established that the AttJ regulator plays a critical role in *attKLM* regulation. *In vivo*, AttJ defect dramatically up-regulated the *attKLM* transcription (Zhang et al., 2004); *in vitro*, purified AttJ specifically bound to two pairs of repeated sequences within the *attK* promoter (Zhang et al., 2002b; Chai et al., 2007). However, the biochemical property and the regulatory mechanism of AttJ both remain poorly understood. In this study, we identified an amino acid that is essential for the function of AttJ and demonstrated that AttJ is regulated in an autorepressive manner. These findings should be informative for further studying the regulatory mechanism of IclR-type regulators.

Materials and Methods

Bacterial strains, plasmids, and growth conditions

The bacterial strains, plasmids used in this study are listed in Table 1. *A. tumefaciens* strains were grown at 28°C in LB medium or in BM minimal medium with mannitol as the sole

Table 1. Bacterial strains and plasmids used in this study

Strain or plasmid	Relevant characteristics ^a	Source or reference
<i>A. tumefaciens</i>		
NT1(<i>traR</i> , <i>tra::lacZ</i> 749)	Also named as CF11, AHL signal indicator strain	Piper et al. (1993)
A6	The wild type octopine strain of <i>A. tumefaciens</i>	A. Kerr
M103	A6 carrying the Tn5 insertion into the <i>attJ</i> gene	Zhang et al. (2002b)
A6MR	A6 carrying Tn5 insertion into the <i>gntR</i> gene and the g300c mutation in the <i>attJ</i> gene, Kan ^r	This study
A6 (Δ <i>gntR</i>)	A6 carrying an in-frame deletion of the <i>gntR</i> gene	This study
A6MR(pLA- <i>gntR</i>)	A6MR carrying the pLA- <i>gntR</i> vector, Kan ^r and Tc ^r	This study
A6 (<i>attJ</i> g300c)	A6 carrying the g300c mutation in the <i>attJ</i> gene	This study
A6 (pLA- <i>attJ::lacZ</i>)	A6 carrying the AttJ transcriptional reporter gene <i>lacZ</i> , Tc ^r	This study
A6 (<i>attJ</i> g300c, pLA- <i>attJ::lacZ</i>)	A6 (<i>attJ</i> g300c) carrying the AttJ transcriptional reporter gene <i>lacZ</i> , Tc ^r	This study
M103(pLA- <i>attJ::lacZ</i>)	M103 carrying the AttJ transcriptional reporter gene <i>lacZ</i> , Tc ^r	This study
A6 (<i>attJ::lacZ</i>)	A6 carrying the <i>attJ</i> gene transcriptionally fused with <i>lacZ</i> , Amp ^r	Zhang et al. (2004)
A6 (<i>attJ::lacZ</i> , pLA- <i>attJ</i>)	A6 (<i>attJ::lacZ</i>) carrying pLA- <i>attJ</i> , Amp ^r and Tc ^r	This study
<i>E. coli</i>		
DH5 α (λ pir)	<i>supE44</i> Δ <i>lacU169</i> (ϕ 80 <i>lacZ</i> Δ M15) <i>hsdR17</i> <i>recA1</i> <i>endA1</i> <i>gyrA96</i> <i>thi-1</i> <i>relA1</i> , λ pir	Laboratory collection
BL21(DE3)	<i>F' ompT hsdS(rB⁻ mB⁻) dcm⁺ Tet^r gal (DE3) endA Hte</i>	Novagen
BW020767(pRL27)	harbouring Tn5 for <i>A. tumefaciens</i> mutagenesis, Kan ^r	Larsen et al. (2002)
Plasmids		
pK18mobsacB	A broad-host-range gene replacement vector; Suc ^r , Kan ^r	Simon et al. (1983)
pK18- <i>attJ</i> g300c	pK18mobsacB harboring an <i>attJ</i> region with the g301c mutation, Kan ^r	This study
pLAFR3	IncP, broad host range cosmid vector, Tc ^r	Staskawicz et al. (1987)
pLA- <i>attJ::lacZ</i>	pLAR3 carrying the <i>attJ</i> gene transcriptionally fused with <i>lacZ</i> in its coding sequence, Tc ^r , Amp ^r	Zhang et al. (2004)
pLA- <i>gntR</i>	pLAFR3 harboring the <i>gntR</i> gene from A6, Tc ^r	This study
pLA- <i>attJ</i>	pLAFR3 harboring the <i>attJ</i> gene from A6, Tc ^r	This study
pET14b- <i>attJ</i>	pET14b vector harboring the encoding region of <i>attJ</i> from A6, Amp ^r	This study
pET14b- <i>attJ</i> g301c	pET14b vector harboring the encoding region of <i>attJ</i> g301c from A6MR, Amp ^r	This study

^aAbbreviations: Amp^r, ampicillin resistant; Kan^r, kanamycin resistant; Tc^r, tetracycline resistant; Suc^r, sucrose resistant.

carbon source and ammonia sulphate as the sole nitrogen source (Zhang and Kerr, 1991). *E. coli* strains were grown at 37°C in LB medium. Antibiotics were added at the following concentrations when required: kanamycin, 50 µg/ml (*A. tumefaciens*) or 100 µg/ml (*E. coli*); tetracycline, 5 µg/ml (*A. tumefaciens*) or 10 µg/ml (*E. coli*); ampicillin, 100 µg/ml; chloramphenicol, 50 µg/ml.

DNA manipulation and plasmid construction

Plasmids and PCR products were purified using Plasmid Miniprep Kit and QIAquick PCR Purification Kit (Qiagen), respectively. For construction of pK18-*gntR*, the DNA fragment flanking *gntR* was amplified from *A. tumefaciens* strain A6 with PCR primer pairs 5'-GCTCTAGAGCGTTGCAA GCTCAAGC-3' / 5'-CGGGATCCGTAGGTGCGCTCAAG CTG-3' and 5'-CGGGATCCAGCGTCGATACAGGTTGC-3' / 5'-GCTCTAGAGCCGTGATAGGGGCTTTC-3' (enzyme cut sites underlined), digested with *Bam*HI and ligated with each other for PCR amplification using primers of 5'-GC TCTAGAGCGTTGCAAAGCTCAAGC-3' and 5'-GCTCTA GAGCCGTGATAGGGGCTTTC-3', the PCR product was purified and cut by *Xba*I for subsequent ligation with *Xba*I-digested vector pK18. The resulting plasmid was screened by PCR and confirmed by DNA sequencing. The plasmid pK18-*attJg301c* was generated by ligation of the *Bam*HI-digested pK18 and the *Bam*HI-digested PCR fragment which was amplified from A6MR with primers of 5'-CGGGATCC ATGGGCCAAAGGGGCCAAG-3' and 5'-CGGGATCCCT AGTCTTTCTGCGATCG-3' (enzyme cut sites underlined).

The constructs pLA-*gntR*, pLA-*traI*, and pLA-*attJ* were assembled as follows: the *GntR*-, *TraI*-, and *AttJ*-coding regions were amplified from *A. tumefaciens* A6 using the PCR primer pairs of 5'-GGAATTCCATGATGGGCGATAGGGA AA-3' / 5'-GGAATTCTCTCCTCACTCCATGC-3', 5'-CG GGATCCATGCTGATTCTGACCGTCTC-3' / 5'-CGGGA TCCTCACGCCGCACTCCTCAAC-3' and 5'-CGGGATC CATGGGCCAAAGGGGCCAAG-3' / 5'-AACTGCAGCTA GTCTTTCTGCGATCGG-3' (enzyme cut sites underlined and translational initiation sites italicized) respectively, digested and linked into the pLAR3 vector. The resultant constructs were further analyzed to ensure that the inserts were in-frame placed in appropriate orientation so that the inserted genes could be driven by the *lac* promoter of pLAR3.

Genetic manipulation of *A. tumefaciens*

A. tumefaciens transformation was carried out by electroporation as reported (McCormac *et al.*, 1998). Tn5 mutagenesis was performed following previous procedures (Zhang *et al.*, 2004). The allelic replacement of *attJg301c* with the native *attJ* in the A6 strain and in-frame deletion of *gntR* were carried out as described previously (Wang *et al.*, 2006a, 2014a).

Quantification of β-galactosidase activity

Quantification of β-galactosidase activity was conducted according to the method previously described (Stachel *et al.*, 1985). The β-galactosidase activity was measured and expressed as units per 10⁹ CFU.

Quantification of AHL and AHL-lactonase activity

The amount of AHL signals produced by bacterial cells was quantitatively determined as described previously using NT1 (*traR*, *tra::lacZ749*) as the indicator strain (Dong *et al.*, 2000). Since AHL is undetectable in the liquid culture of *A. tumefaciens* A6 (Wang *et al.*, 2006a), the AHL production was only quantified on the solid plate in this study. The amount of AHL produced by *A. tumefaciens* was expressed as the equivalent of *N*-(3-oxo-octanoyl)-L-homoserine lactone (3OC8HSL) (Zhang *et al.*, 2002b; Wang *et al.*, 2006a). AHL-lactonase activity was analyzed as previously reported (Dong *et al.*, 2000). Briefly, soluble protein samples were mixed with 3OC8HSL (final concentration, 5 µM) and incubated at 28°C for 20 min. An aliquot of samples was collected for measuring the 3OC8HSL concentration in the reaction mixture.

RNA preparation and RT-PCR

Bacterial cells were cultivated in BM medium at 28°C with 200 rpm shaking, and collected by centrifugation at 4°C. Total RNAs were isolated using RNeasy Mini kit (QIAGEN) and the residual DNA present in the RNA samples was removed by the RNase-free DNase I digestion. Quantity and quality of the RNA samples were monitored by Nanodrop® ND-1000 (Nanodrop Technologies) and agarose gel electrophoresis. An aliquot of 0.2 µg total RNAs was serially 10-time diluted and used as template for one-step RT-PCR analysis (QIAGEN). PCR primer pairs for *attM* and *attJ* were 5'-CTGCCATATTGCGTCGATG-3' / 5'-GTGACGATCT TTGCTCCCTTG-3' and 5'-CTGCCATATTGCGTCGAT G-3' / 5'-GTGACGATCTTTGCTCCCTTG-3', respectively. The primers for *rpoC* (DNA-directed RNA polymerase subunit beta), which was included as control, were 5'-ATCTG GTTCTGAAGTCGCT-3' / 5'-TCGATCACCACGTAGC TCTC-3'.

Transcription start site determination

Identification of the transcription start site of *attJ* was conducted by the method as published previously (Wang *et al.*, 2012, 2014b). Briefly, total RNAs of wild type strain A6 were extracted from bacterial cells cultivated in BM minimal medium and treated with RQ1 RNase-free DNase I (Promega) to remove the residual DNAs. First-stranded cDNA of *attJ* was synthesized from total RNAs by Superscript III reverse transcriptase (Invitrogen) using primers Primer1-*attJ* of 5'-(p)CATCTAAGCGAGTGGGGTCC-3', whose 5'-end has been modified with a phosphorus group (Prologo Company). After the synthesis, the reverse transcriptase was inactivated and the RNAs were digested with RNase Cocktail (Ambion). With purification, cDNAs was then self-ligated by T4 RNA ligase (Roche Molecular Biochemicals) to achieve either self-circularization or intermolecular ligation which was amplified by inverse PCR. The inverse PCR primers were 5'-GA TCAAGCTCAGTCATCACC-3' and 5'-CGATCTGCCGA TGGAACC-3'. After amplification, the PCR products were purified and cloned into pGEM-T easy vector system I (Promega) for DNA sequencing. With sequences analysis, the transcription initiation sites could be mapped to the nucleotide immediately in junction with the 5-(p)-ends of the pri-

mers used for first-strand cDNA synthesis (Fig. 6A).

Protein purification and analysis

His-tagged AttJ purification was carried out as described previously (Zhang *et al.*, 2002b). For purification of the recombinant protein His-tagged AttJ_{D101H}, the *attJ*_{g301c} encoding region from A6MR was amplified and fused into the pET14b vector (Novagen). After sequencing confirmation, the resultant construct of pET14b-*attJ*_{g301c} was transformed into *E. coli* BL21(DE3) by heat shock. The AttJ_{D101H} protein was purified with the Ni-NTA affinity column (Qiagen). Gel filtration was carried out in the DPBS buffer (containing 0.2 g KCl, 0.2 g KH₂PO₄, 8.0 g NaCl, and 2.16 g Na₂HPO₄·7H₂O per L, pH 7.3) with Superdex-75 or Superdex-200 (Amersham). Protein crosslink was performed as follows: the purified proteins were initially desalted with Ultracel-30K (Millipore), and then buffered with a concentration of 150 µg/ml in HGNEED solution (1 mM DTT, 100 mM NaCl, 0.2 mM EDTA, 10% Glycerol, 25 mM HEPES, pH 7.5). The glutaraldehyde solution was prepared in HGNEED buffer with required concentrations, immediately prior to the experiment.

Crosslink was carried out by adding 1 µl of the glutaraldehyde solution to 9 µl of the protein solution and incubating at room temperature. After 12 min, the reaction was quenched with 1 µl of Tris-Glycine solution (1 M Tris, 1 M Glycine, pH 8.0). After boiling for 5 min, samples were analyzed on a 10% PAGE gel, visualized by coomassie blue staining.

Results

Characterization of the AHL-deficient mutant A6MR

To explore regulatory elements associating with QS regulation, we used *A. tumefaciens* A6 as the parent strain for Tn5 mutagenesis to screen AHL-deficient mutants. Among ~6,000 mutants screened, one AHL-deficient mutant, designated as A6MR in this study, was obtained. This mutant produced, if it did, undetectable AHL production on the solid plate, in contrast to the result of its parent A6 (Fig. 1A). Sequence analysis showed the Tn5 transposon inserted within an ORF encoding a *gntR*-family transcriptional factor, sharing 67% identity with the *atu4624* gene in *A. tumefaciens* strain C58. Similar to *atu4624*, the *gntR* gene in A6 was flanked by an upstream gene of *dppB* and a downstream *uxuA*, both of which appeared highly homologous to the *atu4623-atu4626* locus in C58. To validate that the Tn5 insertion is responsible for the AHL-deficient phenotype of A6MR, we firstly transformed the pLA-*gntR* plasmid in the A6 strain for complementation analysis and then in-frame deleted the *gntR* gene in A6 for regeneration of the AHL-deficient phenotype. Unexpectedly, the results showed constitutive expression of *gntR* failed to recover the phenotype and in-frame deletion of *gntR* also was unable to reproduce the phenotype (Fig. 1A), indicating that the AHL-deficiency of A6MR is not attributed to the *gntR* disruption and suggesting that additional mutation(s) may occur in the mutant of A6MR. In search of these mutation(s), we found that the octopine inducer could not promote A6MR to produce detectable AHL, different from the result of the parent strain A6 (Fig. 1B). When TraI was constitutively expressed in A6MR, A6MR(pLA-*traI*) readily produced detectable AHL on solid plates, although its AHL production (10.7±0.3 pmol) appeared less than that of the control A6 (pLA-*traI*) (32.9±5.6 pmol) (Fig. 1B). Interestingly, these characteristics of A6MR seemed to closely parallel with those of the AttJ-mutated M103. As shown in Fig. 1B, no AHL signal was detected for M103 with octopine induction and 10.8±2.7 pmol of AHL could be recorded for the M103(pLA-*traI*) mutant, suggesting that A6MR and M103 may share some overlapping genetic defect(s) for their AHL accumulation. Overexpression of AttM in M103 tempted us to examine the AHL lactonase activity for these bacteria. The results showed the AHL-lactonase activity in A6MR was dramatically higher than that of its parent A6 and comparable to that of M103 (data not shown), indicating that the AHL degradation pathway may implicate with the AHL-deficient phenotype of A6MR.

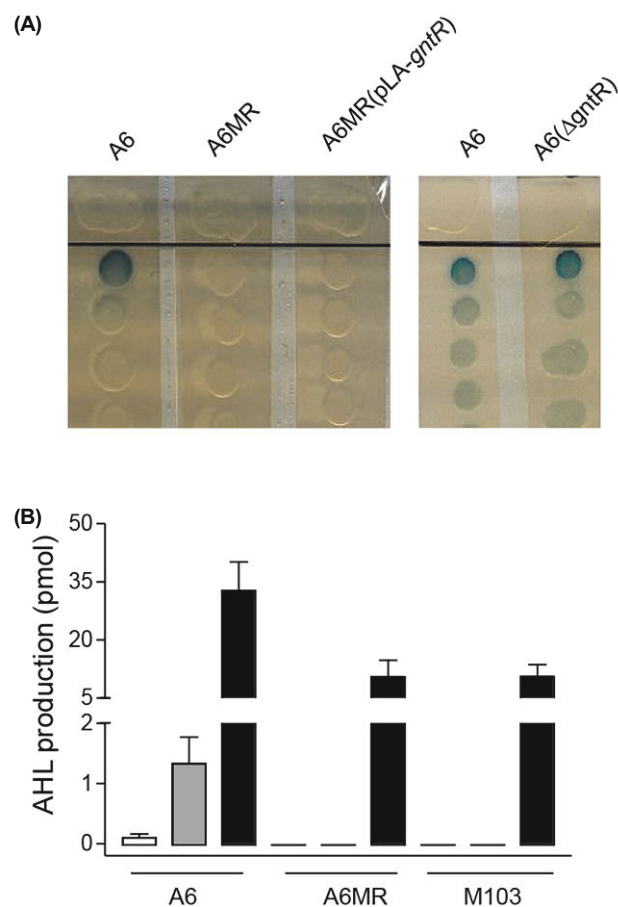


Fig. 1. Identification and characterization of A6 mutant deficient in AHL production. (A) *GntR* is not involved in AHL-deficiency of the mutant of A6 (*gntR*::Tn5). The indicated bacterial strains were grown for 1 d at 28°C to measure their AHL production on minimal medium plates. (B) AHL production of A6MR and its relatives on solid plate. Symbols: open, control; gray, octopine induced; black, constitutive expression of *traI*.

Identification of the *g301c* nucleotide mutation of *attJ* in A6MR

In *A. tumefaciens* A6, the AHL-lactonase activity is predo-

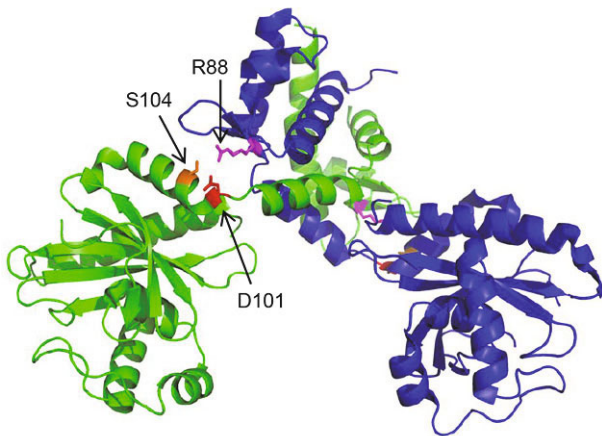


Fig. 2. Location of D101 in the dimer of AttJ by re-analyzing previously published three-dimension crystal structure (Pan *et al.*, 2011). Relevant amino residents are indicated by arrows respectively.

minantly provided by AttM and the *attM* gene is tightly repressed by AttJ. Phenotypic similarity between A6MR and M103 tempted us to sequence the *attM* and *attJ* genes of the A6MR mutant. DNA sequence comparison showed no mutation occurred in the *attM* gene between A6 and A6MR. However, a single point mutation was identified at the position of 301th out of the 825-nucleotide *attJ* encoding region, where a guanine (G) was converted into cytosine (C) in the mutant (data not shown). At amino acid level, the g301c mutation changed an aspartic acid (D) to be a histidine (H) at the 101st position of the AttJ polypeptide. Thus, this point mutation was named as g301c at nucleotide level and D101H at peptide level. Structural modelling suggested that the D101H mutation perched within the swing domain of AttJ, which links the N-terminal HTH DNA binding domain and the C-terminal ligand-binding domain (Fig. 2). In *Thermotoga maritima*, the swing domain of TM-Ic1R, a homologue of AttJ, has been suggested to play a critical role for protein oligomerization, suggesting that the D101H mutation may also affect the folding of AttJ.

D101H affected AttJ dimerization *in vitro*

To test the possibility that D101H may deteriorate the folding of AttJ, we heterogeneously expressed the native AttJ and its variant AttJ_{D101H} in *E. coli*. After purification, the proteins were respectively subjected to gel filtration and protein crosslink to monitor their polymeric status. As shown in Fig. 3A, one peak appeared on the gel filtration graph for the His-tagged AttJ and its molecule weight (MW) was estimated about 60 kDa, doubling the deduced MW of monomeric AttJ and indicating that AttJ may exist as dimer in the DPBS buffer. By contrast, two dominant peaks and one minor peak were observed in the gel filtration graph for His-tagged AttJ_{D101H}; the MWs appeared more than 200 kDa for the predominant peaks and around 60 kDa for the minor peak, indicating that AttJ_{D101H} may aggregate or form oligomers readily under this condition (Fig. 3A). Protein crosslink analysis showed both monomeric and dimeric molecules were captured for AttJ, suggesting AttJ existed as a

dimer in the HGNEB buffer (Fig. 3B). This result appeared compatible with the result of gel filtration in Fig. 3A. In addition to the monomeric and dimeric molecules, however, another molecule species was also captured for AttJ_{D101H} in the protein crosslink experiment (Fig. 3B). The MW of this molecule was within a range of 83 kDa to 175 kDa, suggesting this molecule species may be a tetramer of AttJ_{D101H}. It was noted that the MW of this molecule estimated from the protein crosslink appeared different from that estimated from the gel filtration. This difference of MW may attribute to the different buffers used in the experiment, further supporting that the AttJ_{D101H} variant is less stable compared with the AttJ protein. Put together, these results showed that the D101 amino acid is crucial to stabilize the dimeric status of AttJ *in vitro*.

D101H of AttJ up-regulated *attM* *in vivo*

To further verify that the D101 amino acid is crucial for AttJ function *in vivo*, we regenerated the AttJ_{D101H} mutation in the wild type A6 by allelic replacement. The resultant mutant A6 (*attJ*_{g301c}) failed to produce detectable AHL on solid

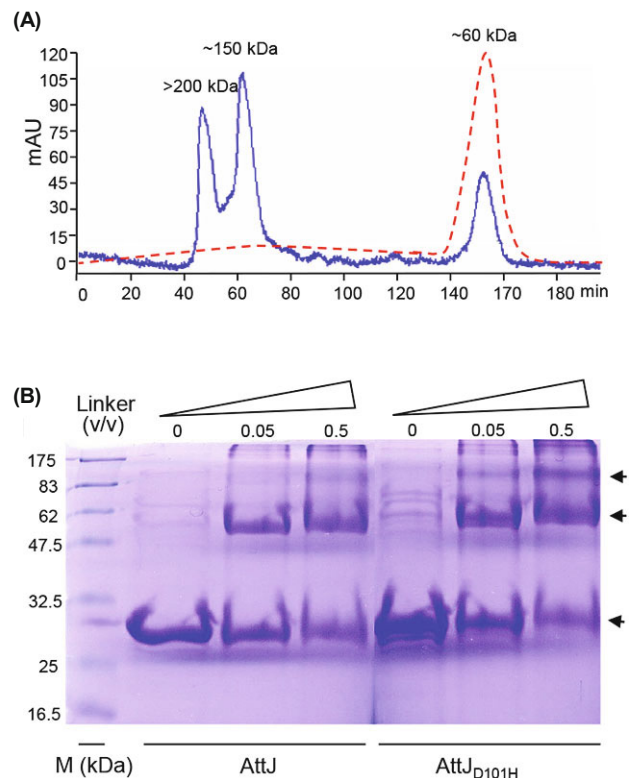


Fig. 3. Effects of D101H mutation on the oligomeric status of AttJ. (A) Gel filtration analysis of native AttJ (red dashed line) and AttJ_{D101H} (blue solid line) with G200 sephadex column in PBS buffer. The estimated molecular weights were indicated on the peaks respectively. (B) Cross-linking of B1cR and AttJ_{D101H} with glutaraldehyde. Protein samples were incubated in the presence of glutaraldehyde with indicated concentrations for 12 min at room temperature and quenched with Tris-Glycine buffer, and then subjected to 10% SDS-PAGE electrophoresis. The protein bands were visualized by staining with coomassie brilliant blue. The bands corresponding to monomer and oligomer molecules are indicated by arrows. M, molecular weight marker.

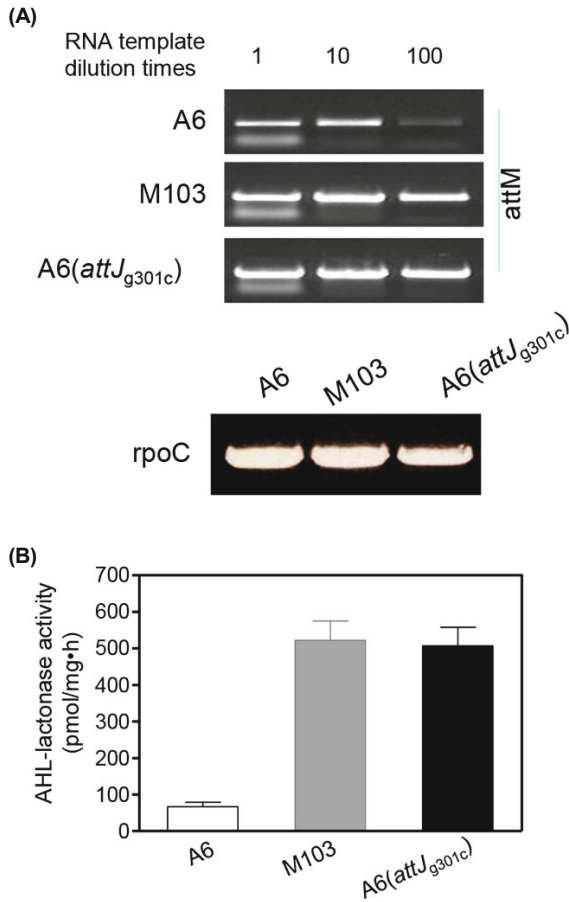


Fig. 4. Overexpression of the AttM AHL-lactonase in A6 (*attJ*_{g301c}). (A) RT-PCR analysis of *attM* transcription. The total RNAs were purified from the given bacterial cultures at exponential phase in minimal media. The RNA templates were serially diluted as indicated on the top for the semi-quantitative RT-PCR analyses. The *rpoC* gene was included as control. (B) AHL-lactonase activities of A6 (*attJ*_{g301c}) and the relevant controls determined by the method described in the context.

plate (data not shown). Hence, the D101H mutation alone could reproduce the phenotypes of A6MR, indicating that the AHL-deficiency of A6MR is due to the D101H mutation of AttJ but not due to the *gntR* disruption. Using A6 (*attJ*_{g301c}), we semi-quantitatively compared the *attM* transcription with those of the wild-type strain A6 and the AttJ-mutated strain M103. As shown in Fig. 4A, RT-PCR results showed *attM* of A6 (*attJ*_{g301c}) was transcribed much more actively than that of A6 and comparable with that of the control M103. Consistently, the AHL lactonase activity in A6 (*attJ*_{g301c}) was significantly higher than that of A6 and indistinguishable from that of M103 (Fig. 4B), demonstrating that the D101H mutation in AttJ could up-regulate the *attM* gene *in vivo*.

D101H of AttJ up-regulated *attJ* *in vivo*

Since AttJ is a key repressor for the *attM* regulation, overexpression of *attM* in A6 (*attJ*_{g301c}) tempted us to examine whether the *attJ* transcription is decreased in this mutant. Unexpectedly, RT-PCR analysis showed that the transcription of *attJ* was highly increased in A6 (*attJ*_{g301c}) compared

to the parent strain A6 (Fig. 5A). To validate this result, the plasmid pLA-*attJ::lacZ*, where the *attJ* gene was transcriptionally fused with the promoterless *lacZ* and thus the *attJ* transcription could be reflected by the β -galactosidase activity, was introduced in A6, A6 (*attJ*_{g301c}) and M103, respectively. As shown in Fig. 5B, the β -galactosidase activity was significantly higher in A6 (*attJ*_{g301c}) than that of A6. Compatible with the RT-PCR result, the β -galactosidase activity in A6 (*attJ*_{g301c}) was comparable to that of M103 (Fig. 5B). Put together, these data not only substantiated that the D101H mutation could fully disarm the function of AttJ, but also suggested that AttJ might also involve in its own transcription.

Identification of transcription start site of *attJ*

For further examination of the *attJ* autoregulation, the promoter regions of *attJ* and *attKLM* were analyzed *in silico* and the transcription start site of *attJ* was identified. As shown in Fig. 7A, 55 base pairs were positioned between the translation start sites of *attJ* and *attK*. The *attKLM* promoter spanned a stretch of DNA sequence from 800 to 884, pre-

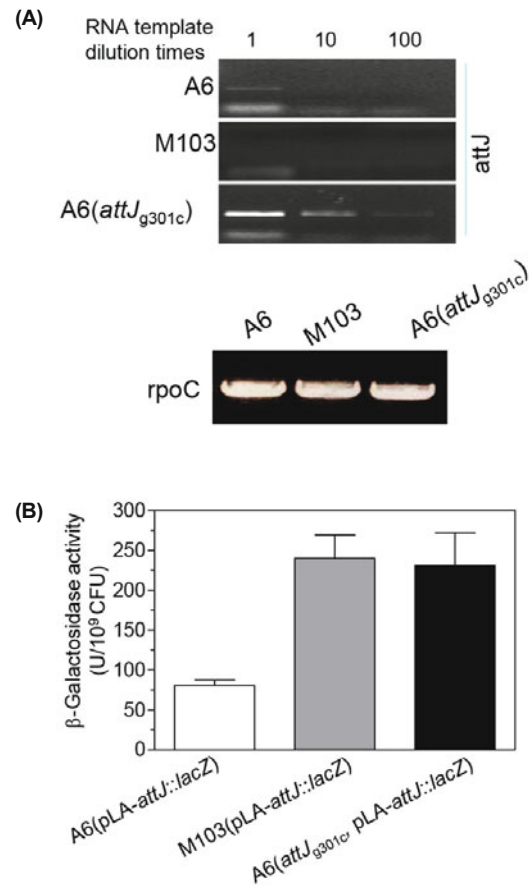


Fig. 5. Overexpression of the AttJ transcriptional factor in A6 (*attJ*_{g301c}). (A) RT-PCR analysis of *attJ* transcription. The total RNAs were purified from the given bacterial cultures at exponential phase in minimal media. The RNA templates were serially diluted as indicated on the top for the semi-quantitative RT-PCR analyses. The *rpoC* gene was included as control. (B) Analysis of the *attJ* transcription in A6 (*attJ*_{g301c}) and its derivatives by determining the β -galactosidase activity at exponential phases.

sumably overlapping the potential promoter of *attJ* (from 829 to 883). At 25 bp upstream of *attJ* translation initiate site, a canonical “-10” element was identified as ACTAAT, which appeared similar to the typical “-10” element (TATAAT) in *E. coli* but different from that of *attK* (CATAGT) in *A. tumefaciens*. The “-35” region of *attJ* predicted as GACCTC, also similar to the typical “-35” element (TTGACA) in *E. coli* and identical to that of *attK*, implying the promoters of *attJ* and *attK* might be recognized by different types of RNA polymerase complex. The transcriptional start site of *attK* identified previously as the T at the 46th position upstream the translation start site of *attK* (Chai *et al.*, 2007). Using a method published previously (Wang *et al.*, 2012), the transcriptional start site of *attJ* was identified as the A at the 16th position upstream the translation start site of *attJ* (Fig. 6).

Autorepressive regulation of AttJ

Analyses of the intergenic region between *attJ* and *attK* also revealed that promoters of *attK* and *attJ* were largely overlapping with each other, and this overlapping region appeared in line with the binding region of AttJ (Fig. 7A). To experimentally validate the autoregulation of AttJ, we utilized two *A. tumefaciens* strains to study the AttJ transcription *in vivo*. One was A6 (*attJ::lacZ*) and the other was A6 (*attJ::lacZ*, pLA-*attJ*). A6 (*attJ::lacZ*) was the wild type strain

A6 whose *attJ* was disrupted by transcriptional fusion of the promoterless *lacZ* fragment. Hence, *attM* was overexpressed and the AHL lactonase activity displayed significantly high (Fig. 7B). A6 (*attJ::lacZ*, pLA-*attJ*) was A6 (*attJ::lacZ*) carrying a low-copy number plasmid where the *attJ* gene was constitutively expressed. Thus, the *attM* was suppressed and the AHL lactonase activity was low (Fig. 7B), suggesting *in trans* expression of *attJ* are functional in *A. tumefaciens*. With these two strains, the *attJ* transcription was analyzed by measuring the β -galactosidase activity. Similar to the *attM* gene, the results indicated that *attJ* was transcribed at a high level in A6 (*attJ::lacZ*) while at a low level in A6 (*attJ::lacZ*, pLA-*attJ*), suggesting that heterogeneous expression of *attJ* could suppress the transcription of *attJ* itself and confirming the autorepression for AttJ regulation.

Discussion

The *attJ-attKLM* cluster is a part of *att* region on the cryptic plasmid of AT in *A. tumefaciens*. Although the *att* region was initially proposed to be involved in attachment to plant, the role of each *att* gene was not fully characterized (Matthysse *et al.*, 2000). In the nopaline-type strain C58, the *attKLM* operon has been well characterized in the metabolism of

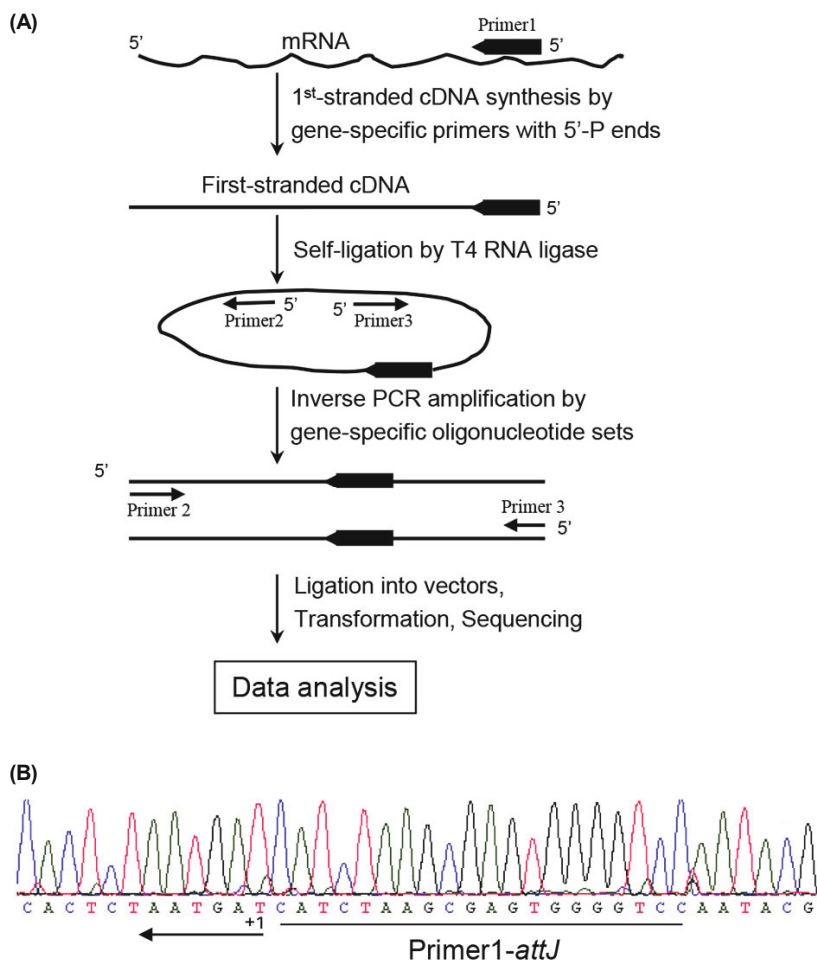


Fig. 6. Determination of *attJ* transcription initiation site. (A) Schematic illustration for determination of transcriptional start site. Primer1 is a 5'-phosphorylated oligonucleotide specific to the gene to be studied, the single-stranded cDNA from the primer extensions is circularized by T4 RNA ligase. Primer2 and Primer3 are normal PCR primers complementary to certain sequences between the Primer1 target and the translational start site. The single-stranded cDNA from primer extensions is circularized by T4 RNA ligase. The inverse PCR using Primer2 and Primer3 and the ligation mixture as template amplify the fragment containing the junction of 3'-end and 5'-end of cDNAs. (B) The transcription start sites for *attJ* in *A. tumefaciens* A6 determined by the strategy above. Only parts of sequence results are presented. Primer1s for *attJ* extension is named as Primer1-*attJ* whose oligonucleotide sequences are underlined respectively; the transcriptional start site is indicated by the starting point of arrow (+1) and the transcriptional direction is represented by the arrow direction.

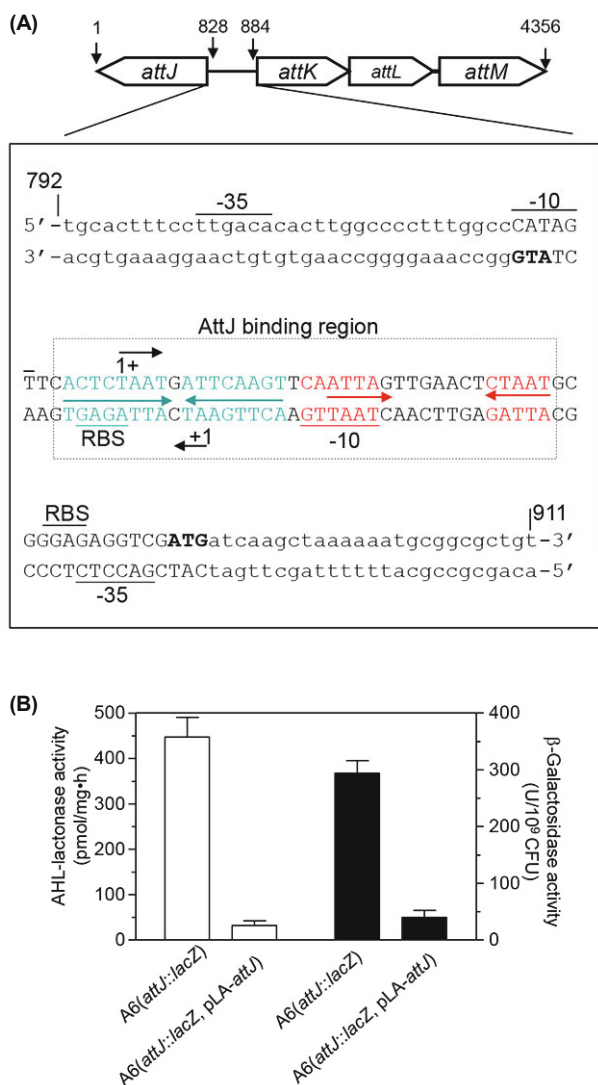


Fig. 7. Autoregulation of AttJ. (A) Schematic presentation of *attJ-attKLM* locus and analysis of intergenic region in *A. tumefaciens* A6. Top: the ORFs are presented on the with the transcription directions indicated with arrows and the translational start sites of *attJ* and *attK* are numbered respectively beginning from the 3rd nucleotide of stop codon for *attJ*. The genes are not drawn in scale relative to each other. Bottom: the DNA sequence is retrieved from GenBank (accession No. AY052389) with the start of 792 and the end of 911 as indicated by vertical arrows. The potential promoter elements of *attKLM*, including -35 region, -10 region and ribosome binding site (SD) are indicated above the sequence, while the corresponding elements for *attJ* promoter are underlined under the sequence. The arrows indicate the direction of transcription and its ends represent the transcription start sites determined in Fig. 6 and Chai et al. (2007). The AttJ binding sites are in boxed in red and blue, and the translation start sites are in bold fonts respectively. (B) Repression of *attJ* and *attM* expression by AttJ. β -Galactosidase activity (left axis) and AHL lactonase activity (right axis) of A6 (*attJ*::*lacZ*) and A6 (*attJ*::*lacZ*, pLA-*attJ*).

gamma-butyrolactone (Carlier et al., 2004; Chai et al., 2007; Subramoni et al., 2014). In octopine-type strain A6, however, studies of the *attJ-attKLM* locus were mainly focused on its significance on QS signal degradation (Zhang et al., 2002b, 2004; Wang et al., 2006b). In both strains, AttJ serves as a negative transcription factor of the *attKLM* operon. In

this study, we showed that the 101st aspartic acid residue (D101) in AttJ is essential for AttJ function, which is conserved in both strains of nopaline-type C58 and octopine-type A6. Conversion of the aspartic acid into a histidine completely abrogates AttJ inhibition, enhancing the AttM expression and leading to the AHL-deficiency phenotype (Figs. 1 and 4). Biochemical evidence suggested D101 is crucial to maintain the dimeric status of AttJ, and substitution of D101 with H in AttJ led to the M103-like phenotypes in *A. tumefaciens* A6, indicating the significance of this amino acid for the biological function of AttJ *in vivo*.

Sequence analyses showed that AttJ is a member of the IclR-family transcription factors. Members of this family typically contain a small N-terminal DNA binding domain, a large C-terminal putative signal binding domain, and a short swing region linking the DAN binding domain and the signal binding domain (Zhang et al., 2002b; Pan et al., 2011, 2013). Usually, IclR-like regulators function as dimers or a dimer of dimers (Molina-Henares et al., 2006). Results from TM-IclR, a homolog of AttJ in *T. maritime*, showed the linking region plays a critical role in protein dimerization. In the crystal structure of TM-IclR, the linking region comprised an α -helix and a short loop, which formed a hydrophobic dimerization interface (Zhang et al., 2002a). In the crystal structure of AttJ, D101 is located right before Helix 5 and its side chain forms two hydrogen bonds with side chain of S104 of the same monomer, and the side chain of S104 is also H-bonded with that of R84 of the other monomer (Fig. 2B). Since D is acidic and negative charged and H is basic and positive charged, D101H mutation may not maintain H-bonding between D101 and S104, thus changing the protein conformation and causing the protein aggregation, although the detailed mechanism remains to be further studied. Identification of D101 as a critical amino acid provides an additional layer of information that how IclR-type repressors function as oligomers to regulate gene expression (Pan et al., 2011, 2013).

In addition to the functional importance of D101 amino acid, we also identified the transcription start site of AttJ and demonstrated that *attJ* is auto-regulated in this paper. Transcription start sites of *attK* and *attJ*, together with the AttJ binding region, suggested the *attJ* and *attK* promoters are overlapping and binding of AttJ may simultaneously occlude the RNA polymerase binding (Fig. 7). Disruption of *attJ* led to considerable increase of its transcription whereas overexpression of *attJ* completely subverted the increase caused by AttJ dysfunction (Fig. 7). These findings are not unique in *A. tumefaciens*; similar autorepression has been elucidated in other members of IclR-type regulators. For example, the *iclR* regulation is repressed by IclR in *E. coli* (Gui et al., 1996a, 1996b) and the *pobR* gene seems to be activated by PobR in *Acinetobacter calcoaceticus* (DiMarco et al., 1993). Since IclR-type usually regulates the carbon metabolism, the autorepression of IclR-type regulators has been suggested to be important for bacterial cells to promptly adjust their physiological status responding to different nutrient sources (Molina-Henares et al., 2006). Serving as an auto-repressor, AttJ may be advantageous for *A. tumefaciens* to defend against the nutrient-depletive conditions. Upon starvation, the QQ system of *A. tumefaciens* has been shown to be active

to terminate the energy-consuming process such as Ti plasmid replication and conjugation (Zhang *et al.*, 2004; Haudecoeur *et al.*, 2009a). To activate the QQ system, *A. tumefaciens* need to induce the *attM* gene and concomitantly reduce the repressive activity of AttJ (Haudecoeur and Faure, 2010). Due to the autorepression of AttJ, induction of *attM* will simultaneously lead to an increase in the transcription of this repressor. Such an increase might be counterproductive, since it would oppose the induction of AttM. In this way, *A. tumefaciens* could induce the expression of *attJ-attKLM* but keep it at an appropriate level when encountering the nutrient depletion. Given that the AttKLM operon is also responsible for the catabolism of γ -butyrolactone, it is of evolutionary advantage to evolve the autoregulatory mechanism for AttJ regulator to cope with the stressful situation during infection (Haudecoeur and Faure, 2010). Together, identification of the point mutation critical for AttJ transcriptional activity and demonstration of its autorepression provide new mechanistic insights into quorum quenching and γ -butyrolactone metabolism in *A. tumefaciens*.

In conclusion, AttJ is an important transcription factor regulating the expression of AttKLM operon. In *A. tumefaciens*, AttKLM have been identified as enzymes degrading host-produced GABA and bacteria-derived quorum sensing signals. Thus studies of AttJ-mediated AttKLM regulation are of significance to understand the tumorigenicity of *A. tumefaciens*. Using a Tn5-based mutagenesis approach, in this study we demonstrated the D101 of AttJ plays a critical role in the transcription activity of AttJ, most likely by supporting the protein oligomeric status. Also, we revealed the transcription of *attJ* is regulated through a negative feedback loop. Mutation of D101H both increased the expression of *attKLM* and *attJ* itself as well. Put together, these results not only expand our understanding on the biochemical property of AttJ but also provide new mechanistic insights into the regulation of GABA metabolism and quorum quenching of *A. tumefaciens*.

Acknowledgements

This work was financially supported by the Biomedical Research Council, Agency of Science, Technology and Research (A*STAR, Singapore) and Singapore National Research Foundation NRF-RF2009-RF001-267 (YGG).

References

- Bell, K.S., Sebahia, M., Pritchard, L., Holden, M.T., Hyman, L.J., Holeva, M.C., Thomson, N.R., Bentley, S.D., Churcher, L.J., Mungall, K., *et al.* 2004. Genome sequence of the enterobacterial phytopathogen *Erwinia carotovora* subsp. *atroseptica* and characterization of virulence factors. *Proc. Natl. Acad. Sci. USA* **101**, 11105–11110.
- Bertani, I., Kojic, M., and Venturi, V. 2001. Regulation of the *p*-hydroxybenzoic acid hydroxylase gene (*pobA*) in plant-growth-promoting *Pseudomonas putida* WCS358. *Microbiology* **147**, 1611–1620.
- Carlier, A., Chevrot, R., Dessaux, Y., and Faure, D. 2004. The assimilation of gamma-butyrolactone in *Agrobacterium tumefaciens* C58 interferes with the accumulation of the *N*-acyl-homoserine lactone signal. *Mol. Plant Microbe Interact.* **17**, 951–957.
- Chai, Y., Tsai, C.S., Cho, H., and Winans, S.C. 2007. Reconstitution of the biochemical activities of the AttJ repressor and the AttK, AttL, and AttM catabolic enzymes of *Agrobacterium tumefaciens*. *J. Bacteriol.* **189**, 3674–3679.
- Chevrot, R., Rosen, R., Haudecoeur, E., Cirou, A., Shelp, B.J., Ron, E., and Faure, D. 2006. Gaba controls the level of quorum-sensing signal in *Agrobacterium tumefaciens*. *Proc. Natl. Acad. Sci. USA* **103**, 7460–7464.
- DiMarco, A.A., Averhoff, B., and Ornston, L.N. 1993. Identification of the transcriptional activator *pobR* and characterization of its role in the expression of *pobA*, the structural gene for *p*-hydroxybenzoate hydroxylase in *Acinetobacter calcoaceticus*. *J. Bacteriol.* **175**, 4499–4506.
- Dong, Y.H., Xu, J.L., Li, X.Z., and Zhang, L.H. 2000. AiiA, an enzyme that inactivates the acylhomoserine lactone quorum-sensing signal and attenuates the virulence of *Erwinia carotovora*. *Proc. Natl. Acad. Sci. USA* **97**, 3526–3531.
- Grainger, D.C., Overton, T.W., Reppas, N., Wade, J.T., Tamai, E., Hobman, J.L., Constantinidou, C., Struhl, K., Church, G., and Busby, S.J. 2004. Genomic studies with *Escherichia coli* MelR protein: Applications of chromatin immunoprecipitation and microarrays. *J. Bacteriol.* **186**, 6938–6943.
- Gui, L., Sunnarborg, A., and LaPorte, D.C. 1996. Regulated expression of a repressor protein: FadR activates *iclR*. *J. Bacteriol.* **178**, 4704–4709.
- Gui, L., Sunnarborg, A., Pan, B., and LaPorte, D.C. 1996. Autoregulation of *iclR*, the gene encoding the repressor of the glyoxylate bypass operon. *J. Bacteriol.* **178**, 321–324.
- Haudecoeur, E. and Faure, D. 2010. A fine control of quorum-sensing communication in *Agrobacterium tumefaciens*. *Commun. Integr. Biol.* **3**, 84–88.
- Haudecoeur, E., Planamente, S., Cirou, A., Tannieres, M., Shelp, B.J., Morera, S., and Faure, D. 2009a. Proline antagonizes GABA-induced quenching of quorum-sensing in *Agrobacterium tumefaciens*. *Proc. Natl. Acad. Sci. USA* **106**, 14587–14592.
- Haudecoeur, E., Tannieres, M., Cirou, A., Raffoux, A., Dessaux, Y., and Faure, D. 2009b. Different regulation and roles of lactonases AiiB and AttM in *Agrobacterium tumefaciens* C58. *Mol. Plant Microbe Interact.* **22**, 529–537.
- Krell, T., Molina-Henares, A.J., and Ramos, J.L. 2006. The IclR family of transcriptional activators and repressors can be defined by a single profile. *Protein Sci.* **15**, 1207–1213.
- Larsen, R.A., Wilson, M.M., Guss, A.M., and Metcalf, W.W. 2002. Genetic analysis of pigment biosynthesis in *Xanthobacter autotrophicus* Py2 using a new, highly efficient transposon mutagenesis system that is functional in a wide variety of bacteria. *Arch. Microbiol.* **178**, 193–201.
- Matthysse, A.G., Yarnall, H., Boles, S.B., and McMahan, S. 2000. A region of the *Agrobacterium tumefaciens* chromosome containing genes required for virulence and attachment to host cells. *Biochim. Biophys. Acta.* **1490**, 208–212.
- McCormac, A.C., Elliott, M.C., and Chen, D.F. 1998. A simple method for the production of highly competent cells of *Agrobacterium* for transformation via electroporation. *Mol. Biotechnol.* **9**, 155–159.
- Molina, M.L., Barrera, F.N., Fernandez, A.M., Poveda, J.A., Renart, M.L., Encinar, J.A., Riquelme, G., and Gonzalez-Ros, J.M. 2006. Clustering and coupled gating modulate the activity in KcsA, a potassium channel model. *J. Biol. Chem.* **281**, 18837–18848.
- Molina-Henares, A.J., Krell, T., Eugenia Guazzaroni, M., Segura, A., and Ramos, J.L. 2006. Members of the IclR family of bacterial transcriptional regulators function as activators and/or repressors. *FEMS Microbiol. Rev.* **30**, 157–186.
- Pan, Y., Fiscus, V., Meng, W., Zheng, Z., Zhang, L.H., Fuqua, C., and Chen, L. 2011. The *Agrobacterium tumefaciens* transcription

- factor BlcR is regulated via oligomerization. *J. Biol. Chem.* **286**, 20431–20440.
- Pan, Y., Wang, Y., Fuqua, C., and Chen, L. 2013. *In vivo* analysis of DNA binding and ligand interaction of BlcR, an IclR-type repressor from *Agrobacterium tumefaciens*. *Microbiology* **159**, 814–822.
- Pappas, K.M. and Winans, S.C. 2003. A LuxR-type regulator from *Agrobacterium tumefaciens* elevates Ti plasmid copy number by activating transcription of plasmid replication genes. *Mol. Microbiol.* **48**, 1059–1073.
- Piper, K.R., Beck von Bodman, S., and Farrand, S.K. 1993. Conjugation factor of *Agrobacterium tumefaciens* regulates Ti plasmid transfer by autoinduction. *Nature* **362**, 448–450.
- Rutherford, S.T. and Bassler, B.L. 2012. Bacterial quorum sensing: Its role in virulence and possibilities for its control. *Cold Spring Harbor Perspect. Med.* **2**, a012427.
- Simon, R., Priefer, U., and Pühler, A. 1983. A broad host range mobilization system for *in vivo* genetic engineering: Transposon mutagenesis in Gram-negative bacteria. *Bio/Technology* **1**, 784–791.
- Stachel, S.E., An, G., Flores, C., and Nester, E.W. 1985. A Tn3 lacZ transposon for the random generation of beta-galactosidase gene fusions: Application to the analysis of gene expression in *Agrobacterium*. *EMBO J.* **4**, 891–898.
- Staskawicz, B., Dahlbeck, D., Keen, N., and Napoli, C. 1987. Molecular characterization of cloned avirulence genes from race 0 and race 1 of *Pseudomonas syringae* pv. *glycinea*. *J. Bacteriol.* **169**, 5789–5794.
- Subramoni, S., Nathoo, N., Klimov, E., and Yuan, Z.C. 2014. *Agrobacterium tumefaciens* responses to plant-derived signaling molecules. *Front. Plant Sci.* **5**, 322.
- Sunnarborg, A., Klumpp, D., Chung, T., and LaPorte, D.C. 1990. Regulation of the glyoxylate bypass operon: Cloning and characterization of iclR. *J. Bacteriol.* **172**, 2642–2649.
- Wang, C., Lee, J., Deng, Y., Tao, F., and Zhang, L.H. 2012. ARF-TSS: An alternative method for identification of transcription start site in bacteria. *Biotechniques* **2012**, 1–3.
- Wang, C., Yan, C., Fuqua, C., and Zhang, L.H. 2014a. Identification and characterization of a second quorum-sensing system in *Agrobacterium tumefaciens* A6. *J. Bacteriol.* **196**, 1403–1411.
- Wang, C., Ye, F., Kumar, V., Gao, Y.G., and Zhang, L.H. 2014b. BswR controls bacterial motility and biofilm formation in *Pseudomonas aeruginosa* through modulation of the small RNA *rsmZ*. *Nucleic Acids Res.* **42**, 4563–4576.
- Wang, C., Zhang, H.B., Chen, G., Chen, L., and Zhang, L.H. 2006a. Dual control of quorum sensing by two tram-type antiactivators in *Agrobacterium tumefaciens* octopine strain A6. *J. Bacteriol.* **188**, 2435–2445.
- Wang, C., Zhang, H.B., Wang, L.H., and Zhang, L.H. 2006b. Succinic semialdehyde couples stress response to quorum-sensing signal decay in *Agrobacterium tumefaciens*. *Mol. Microbiol.* **62**, 45–56.
- Waters, C.M. and Bassler, B.L. 2005. Quorum sensing: Cell-to-cell communication in bacteria. *Annu. Rev. Cell Dev. Biol.* **21**, 319–346.
- White, C.E. and Winans, S.C. 2007. Cell-cell communication in the plant pathogen *Agrobacterium tumefaciens*. *Philos. Trans R. Soc. Lond B Biol. Sci.* **362**, 1135–1148.
- Zhang, L.H. and Kerr, A. 1991. A diffusible compound can enhance conjugal transfer of the TI plasmid in *Agrobacterium tumefaciens*. *J. Bacteriol.* **173**, 1867–1872.
- Zhang, R.G., Kim, Y., Skarina, T., Beasley, S., Laskowski, R., Arrow-smith, C., Edwards, A., Joachimiak, A., and Savchenko, A. 2002a. Crystal structure of *Thermotoga maritima* 0065, a member of the IclR transcriptional factor family. *J. Biol. Chem.* **277**, 19183–19190.
- Zhang, L., Murphy, P.J., Kerr, A., and Tate, M.E. 1993. *Agrobacterium* conjugation and gene regulation by N-acyl-L-homoserine lactones. *Nature* **362**, 446–448.
- Zhang, H.B., Wang, L.H., and Zhang, L.H. 2002b. Genetic control of quorum-sensing signal turnover in *Agrobacterium tumefaciens*. *Proc. Natl. Acad. Sci. USA* **99**, 4638–4643.
- Zhang, H.B., Wang, C., and Zhang, L.H. 2004. The quorumone degradation system of *Agrobacterium tumefaciens* is regulated by starvation signal and stress alarmone (p)ppGpp. *Mol. Microbiol.* **52**, 1389–1401.